This journal is © The Royal Society of Chemistry 2017

Electronic Supplementary Material (ESI 1-3)

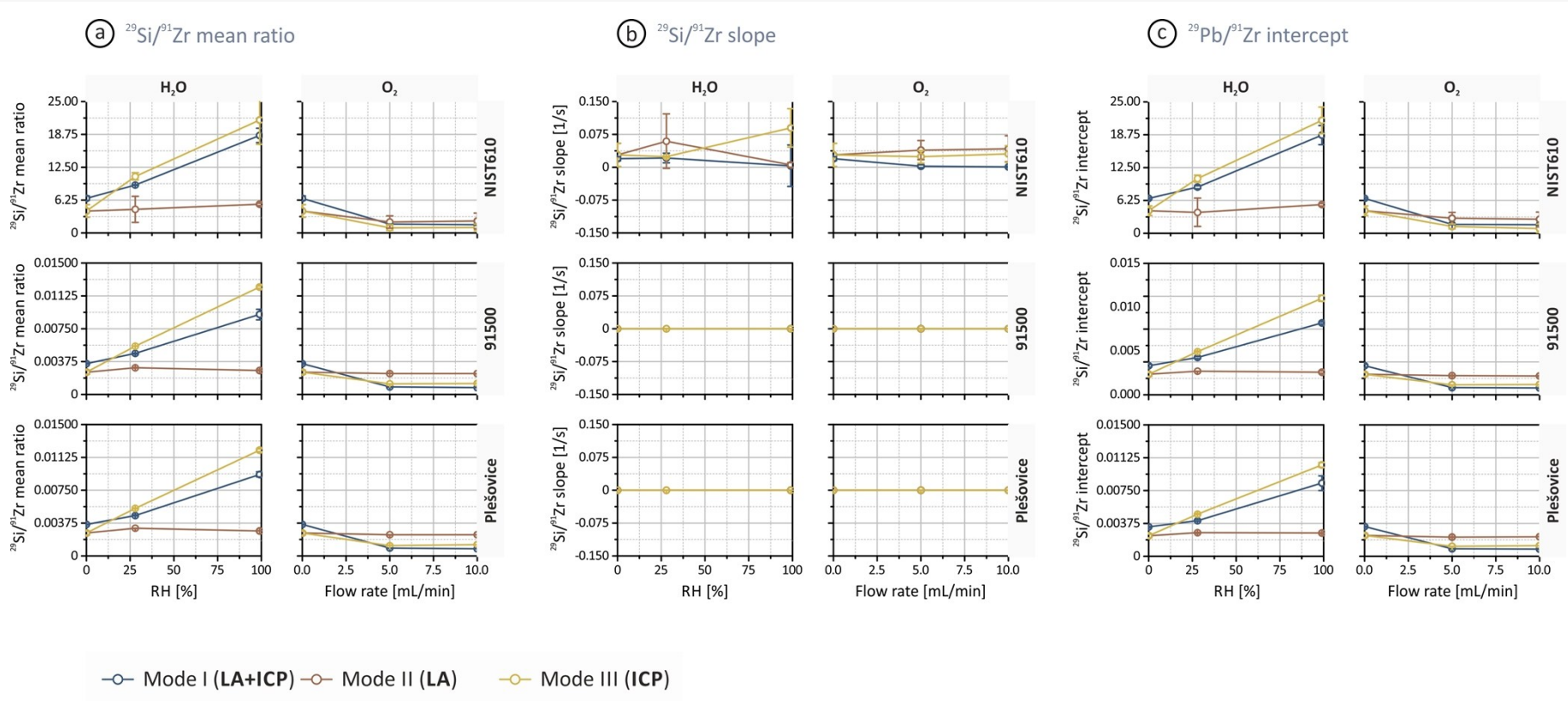

Figure E1: $^{29}Si/^{91}Zr$ data acquired by LA-ICP(Q)MS of NIST SRM610 and 91500 & Plešovice zircons using He + H_2O or O_2 carrier gases at a glance. Panel (a): $^{29}Si/^{91}Zr$ mean intensity ratios averaged over an acquisition timeframe of 53 s. Panel (b): Slopes b of linear regression curves calculated from $^{29}Si/^{91}Zr$ point-by-point signal ratios according to expression (1). Panel (c): Intercepts a of linear regression curves calculated from $^{29}Si/^{91}Zr$ point-by-point signal ratios according to expression (1). All data points represent the mean of 3 to 12 measurements and error bars refer to the 95 % confidence interval of the mean. This figure is organized as follows: Each of the panels (a), (b), and (c) contains three subsets of plots which are arranged pairwise referring to one sample-carrier gas combination. These subsets are, furthermore, consistently scaled for better comparability. For example, mean $^{29}Si/^{91}Zr$ ratios determined for NIST SRM610 are shown in panel (a) top left while corresponding intercepts are displayed in panel (c) top right. Slopes of $^{29}Si/^{91}Zr$ ratios *vs.* time shown in panel (b) were equally scaled throughout all subsets to allow conclusion on the degree of down-hole fractionation in dependence on the material.

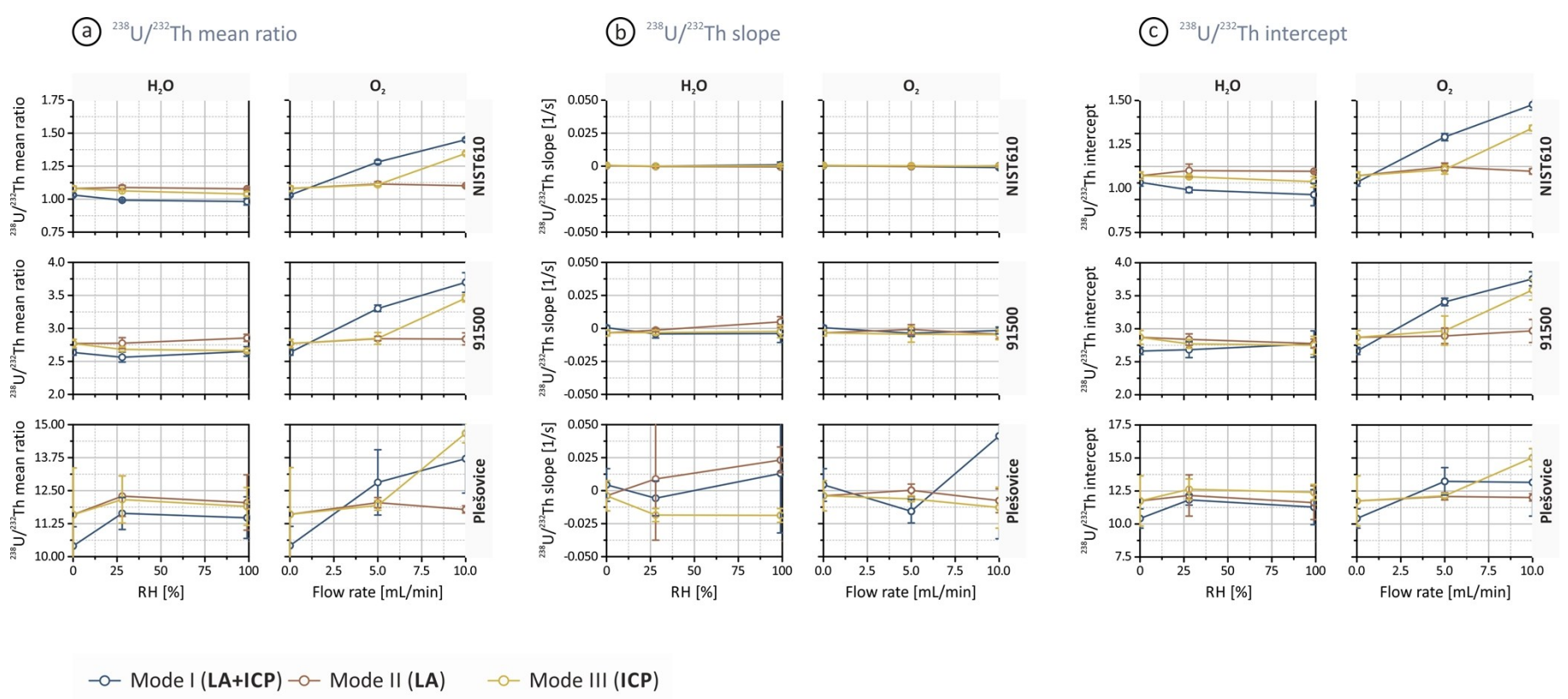

Figure E2: $^{238}U/^{232}Th$ data acquired by LA-ICP(Q)MS of NIST SRM610 and 91500 & Plešovice zircons using He + H_2O or O_2 carrier gases at a glance. Panel (a): $^{238}U/^{232}Th$ mean intensity ratios averaged over an acquisition timeframe of 53 s. Panel (b): Slopes b of linear regression curves calculated from $^{238}U/^{232}Th$ point-by-point signal ratios according to expression (1). Panel (c): Intercepts a of linear regression curves calculated from $^{238}U/^{232}Th$ point-by-point signal ratios according to expression (1). All data points represent the mean of 3 to 12 measurements and error bars refer to the 95 % confidence interval of the mean. This figure is organized as follows: Each of the panels (a), (b), and (c) contains three subsets of plots which are arranged pairwise referring to one sample-carrier gas combination. These subsets are, furthermore, consistently scaled for better comparability. For example, mean $^{238}U/^{232}Th$ ratios determined for NIST SRM610 are shown in panel (a) top left while corresponding intercepts are displayed in panel (c) top right. Slopes of $^{238}U/^{232}Th$ ratios *vs.* time shown in panel (b) were equally scaled throughout all subsets to allow conclusion on the degree of down-hole fractionation in dependence on the material.

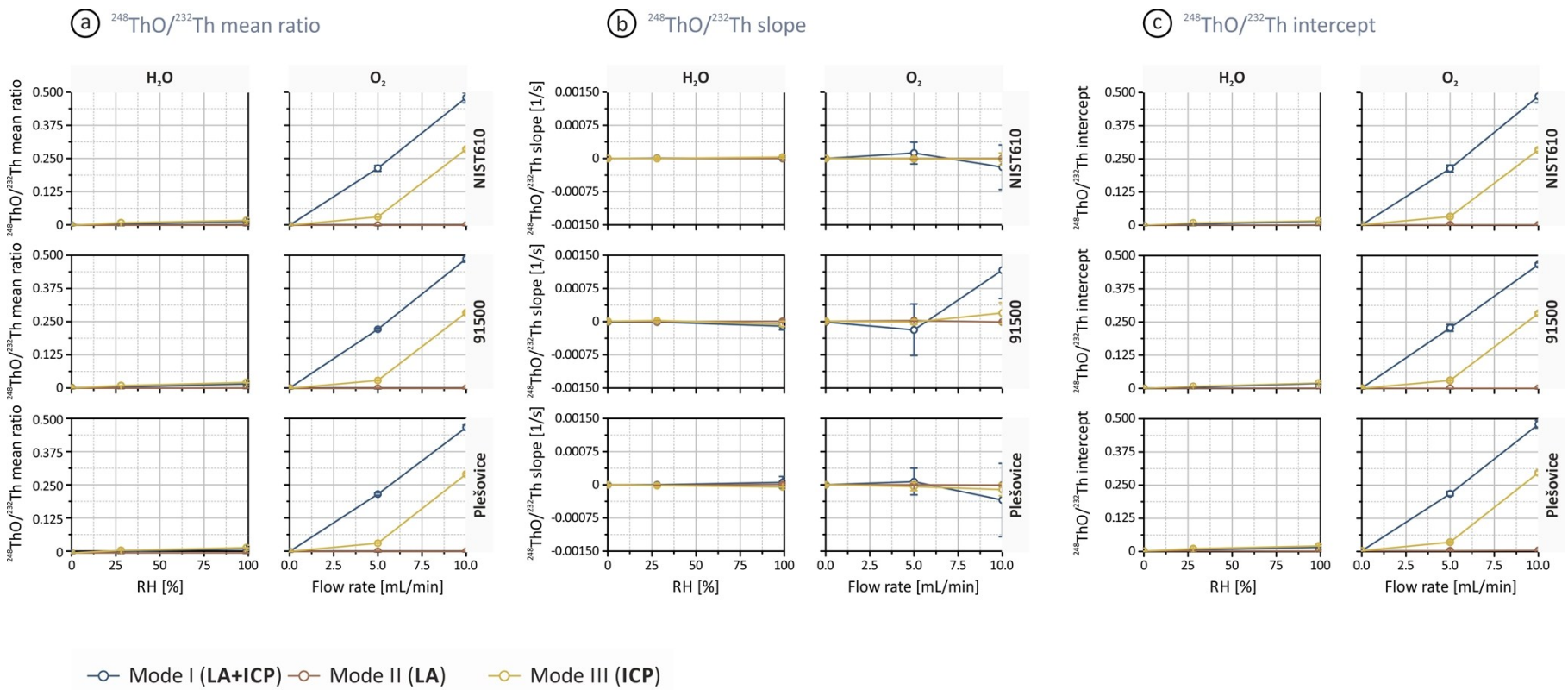

Figure E3: $^{248}ThO/^{232}Th$ data acquired by LA-ICP(Q)MS of NIST SRM610 and 91500 & Plešovice zircons using He + H_2O or O_2 carrier gases at a glance. Panel (a): $^{248}ThO/^{232}Th$ mean intensity ratios averaged over an acquisition timeframe of 53 s. Panel (b): Slopes b of linear regression curves calculated from $^{248}ThO/^{232}Th$ point-by-point signal ratios according to expression (1). Panel (c): Intercepts a of linear regression curves calculated from $^{248}ThO/^{232}Th$ point-by-point signal ratios according to expression (1). All data points represent the mean of 3 to 12 measurements and error bars refer to the 95 % confidence interval of the mean. This figure is organized as follows: Each of the panels (a), (b), and (c) contains three subsets of plots which are arranged pairwise referring to one sample-carrier gas combination. These subsets are, furthermore, consistently scaled for better comparability. For example, mean $^{248}ThO/^{232}Th$ ratios determined for NIST SRM610 are shown in panel (a) top left while corresponding intercepts are displayed in panel (c) top right. Slopes of $^{248}ThO/^{232}Th$ ratios *vs.* time shown in panel (b) were equally scaled throughout all subsets to allow conclusion on the degree of down-hole fractionation in dependence on the material.